Chinese Chemical Letters 33 (2022) 1505–1510

Contents lists available at ScienceDirect

Chinese Chemical Letters

journal homepage: www.elsevier.com/locate/cclet

Pseudo-crown ether having AIE and PET effects from a TPE-CD conjugate for highly selective detection of mercury ions

Kai-Ran Zhang[a], Ming Hu[a], Jun Luo[b], Fengying Ye[a], Ting-Ting Zhou[a], Ying-Xue Yuan[a], Miao-Li Gao[a], Yan-Song Zheng[a,*]

[a] *Key Laboratory of Material Chemistry for Energy Conversion and Storage, Ministry of Education, School of Chemistry and Chemical Engineering, Huazhong University of Science and Technology, Wuhan 430074, China*
[b] *Tongji School of Pharmacy, Huazhong University of Science and Technology, Wuhan 430030, China*

ARTICLE INFO

Article history:
Received 27 June 2021
Revised 10 August 2021
Accepted 13 August 2021
Available online 19 August 2021

Keywords:
Tetraphenylethylene-cyclodextrin conjugate
Aggregation-induced emission
Self-inclusion compound
Photo-induced electron transfer
Mercury ion sensor
Highly selective
Pseudo-crown ether

ABSTRACT

A new tetraphenylethylene-cyclodextrin (TPE-CD) conjugate with a linkage composed of long triethylene glycol chain and triazole ring on the CD rim has been designed and synthesized. The TPE-CD conjugate exists in a stretched form in DMSO and enhances its fluorescence after addition of a small amount of water due to aggregation-induced emission (AIE) effect. However, in the presence of a large amount of water, the TPE unit will enter the cyclodextrin cavity to form a folded self-inclusion compound. In the self-inclusion compound, not only nitrogen-containing *pseudo*-crown ether is formed but also arouses photo-induced electron transfer (PET) process from nitrogen atoms of triazole ring to TPE unit and quenches the fluorescence although more aggregation occurs in more water. This is the first finding that TPE-macrocycle conjugate can form *pseudo*-crown ether and has both the AIE phenomenon and the PET effect. Interestingly, only mercury ion arouses the fluorescence recover of the self-inclusion compound by entering the *pseudo*-crown ether cavity and blocking the PET process by binding to the nitrogen atoms, while other tested metal ions almost have no effect on the fluorescence. Therefore, the TPE-CD conjugate can be used for the highly selective fluorescence "Turn-On" detection of Hg^{2+}.

Metal ions have critical impact on environment, living systems, and health of human. Among the metal ions, mercury ion is especially harmful and it is very important to detect it and track its source. Although a large number of analysis methods have been reported, to develop highly selective reagents for the detection of mercury ions is still a challenge.

Aggregation-induced emission (AIE) phenomenon has become one of the most top research frontiers in chemistry and materials area due to great application potential in solid emitter, sensors, biological imaging, and so on [1–7]. The combination of AIE molecules with host macrocycle compounds [8] such as crown ether, cyclodextrin (CD), calixarene, and cucurbituril will monitor *in situ* the process of loading, delivering, transferring, releasing and self-assembling of these host compounds toward guest molecules, and develop novel emitting materials and sensors, due to the fluorescence change of AIE molecules inside and outside the cavity of host macrocycle compounds. Truly, some exceptional results have been obtained in AIE host-guest chemistry.

For example, Wang *et al.* connected benzo-15-crown-5 ether onto each phenyl ring of tetraphenylethylene (TPE) core and the obtained TPE-crown could be used as K(I)-catching tentacles [9]. Bearing bigger crown ether rings, TPE-crown compounds could include ammonium [10,11], sense folic acid [12] and load anti-cancer molecules [13]. By click reaction, a prepared triazole bridged AIE active cyclodextrin probe was used in specific detection of Cd^{2+}, exhibiting an excellent selective turn-on fluorescence response to Cd^{2+} in neutral environments [14]. Based on AIE effects and host-guest recognition of nitrophenol with cyclodextrin, sensitive detection of β-galactosidase was carried out [15]. Recently, AIE donors self-assembled with cyclodextrin bearing rhodamine B fluorophore could form a platform for mimicking light-harvesting system [16]. Outstandingly, by the host-guest chemistry of cyclodextrin and AIE, reaction kinetics was even visualized by the fluorescence change of AIE molecules in different cyclodextrins [17]. In addition, through inclusion and assembly of AIE molecules with calixarenes and cucurbituril, some AIE host-guest systems with excellent application property are also set up. Through including TPE ammoniums into the cavity of calixarenes, making fluorescence enhancement and cytotoxicity attenuation, the supramolecular assembly

* Corresponding author.
E-mail address: zh907@hust.edu.cn (Y.-S. Zheng).

https://doi.org/10.1016/j.cclet.2021.08.072
1001-8417/

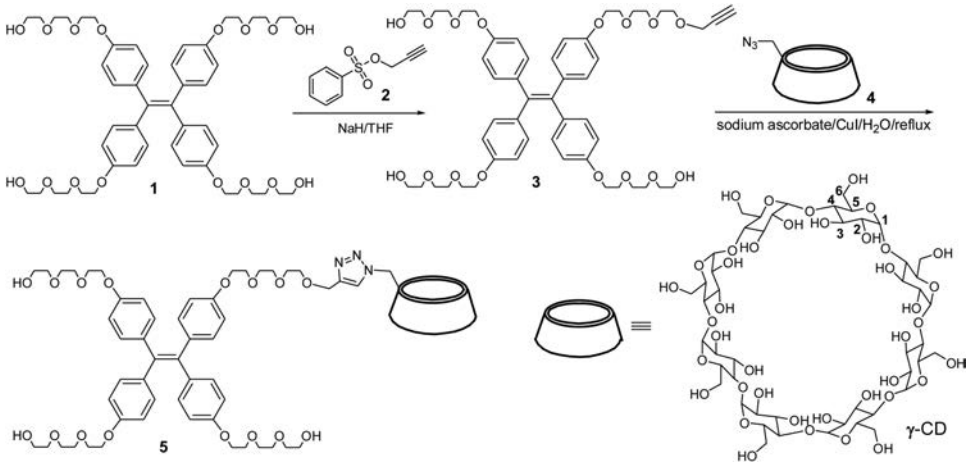

Fig. 1. Synthetic route of TPE-CD conjugate **5**.

of TPE-calixarenes could be served as precise phototheranostics [18] and a superior fluorescent bioprobe for cancer surgery [19]. TPE bearing four pentaethylene glycol pyridiniums could be co-assembled with cucurbit[6]urile and make the fluorescence enhancement but the enhanced fluorescence could be attenuated by addition of spermine and spermidine, showing potential for detection of biogenic amines [20]. Using molecule handcuffs cucurbit[8]urile, two-dimensional supramolecular organic framework (2D SOF) could be produced by interaction with Brooker's merocyanine analogues that could act as a tracker for the nucleus [21].

Although great achievements on the integration of AIE phenomenon with host-guest chemistry have been made, the research reports about this subject are few compared with the rapid growth of AIE researches. Previously, we found that TPE derivatives bearing polyethylene glycol could be included by γ-cyclodextrin and formed stable complex in water [22]. If the TPE polyethylene glycol is connected to γ-cyclodextrin by covalent bonds, the resultant CD-cyclodextrin conjugate should display some interesting AIE host-guest properties. Here we report that the synthesis, self-inclusion, formation of *pseudo*-crown ether formation of the CD-cyclodextrin conjugate, and its application in highly selective detection of mercury ions due to synergistic effect of AIE and photo-induced electron transfer (PET) phenomena.

As shown in Fig. 1, the nucleophilic substitution of propargyl benzenesulfonate **2** with large excess amount of TPE tetratriethylene glycol **1** produced TPE tetratriethylene glycol monopropyne **3**. Then a copper-catalyzed click reaction of the terminal alkyne **3** with γ-CD azide **4** furnished a TPE-CD conjugate **5** bearing triazole ring on CD rim in 80% yield. The conjugate was fully characterized by ^{1}H and ^{13}C NMR, HRMS, and IR spectra. Although triethylene glycol chains and CD unit are hydrophilic, the conjugate is difficult to dissolve in water. There is a small solubility in DMSO and DMF, but it is almost insoluble in other convenient organic solvent.

As solid powder, conjugate **5** emitted strong sky blue light under irradiation of 365 nm light. Its solution in DMSO also showed strong fluorescence and the fluorescence intensity gradually decreased with dilution (Figs. S13–S15 in Supporting information). This indicated that the conjugate kept the AIE characters of TPE unit. By making use of integrate sphere measurement, the absolute fluorescence quantum yield (Φ_f) of solid powder and solution of **5** in DMSO was 18.04% and 1.18%, respectively, also demonstrating the AIE enhancement effect. Unexpectedly, when the DMSO solution of **5** was gradually added by water, the fluorescence intensity was not always increased with water fraction. In less than 40% water fraction (volume percentage, the same below), fluorescence intensity increased with the water fraction. But in larger than 40% water fraction, the intensity decreased with continuous addition of water and even decreased to the same intensity of DMSO solution after 90% water was added (Figs. 2A and B). This phenomenon is very rare for AIE compounds. In some AIE tests, when bad solvent was added in very high fraction (more than 90%), the fluorescent intensity is not continued to increase, instead, start to decrease due to change of aggregates structure or/and morphology. But the decline is very little and the emission is still much stronger than that in solution without bad solvent. The absolute Φ_f of solution of **5** in DMSO/H_2O at 100:0, 80:20, 60:40, 40:60 and 10:90 was 1.18%, 2.01%, 2.70%, 2.39% and 1.19%, respectively, which was in accordance with the change of fluorescent spectra. The Φ_f in DMSO/H_2O 10:90 also decreased to that in pure DMSO. This is very abnormal. Meanwhile, the emission maximum wavelength showed a gradually hypsochromic shift with water fraction (Fig. 2C). Moreover, at about 40% water fraction, the emission wavelength decreased most rapidly. In addition, absorption spectra also displayed gradually hypsochromic shift at about 325 nm with water fraction (Fig. 2D), which was in accordance with the wavelength change of emission spectra.

For knowing whether there was inclusion of TPE unit into the cavity of CD when water was added, the ^{1}H NMR spectra of conjugate **5** in a mixed solvent of DMSO-d_6/D_2O with different water fraction were measured. As shown in Fig. 3, the signals of the phenyl protons of TPE gradually moved upfield with water fraction. After 90% water was added, one pair of doublets of the phenyl rings got a shift of 0.056 and 0.159 ppm, respectively. Accompanying upfield shift, the pair of doublets were divided into at least three pairs of doublets, indicating that the four phenyl rings of the TPE unit were in complete different environment. Meanwhile, the proton of triazole also had an upfield shift from 8.024 ppm to 7.763 ppm and got a shift of 0.261 ppm after 90% water was added. The upfield shift of the protons of both the phenyl rings and triazole demonstrated that triazole proton was in the shielding area of phenyl ring, and phenyl protons were also in the shielding area of triazole ring. In addition, the H_1 signal of CD marocycle was shifted to lowfield while the proton signals of OH_2, OH_3 and OH_6 disappeared due to proton interchange between hydroxyl groups and D_2O. This NMR measurement corroborated that the TPE unit was included into the cavity of CD and was close to the triazole ring on the narrow rim of CD.

In the 2D NMR NOESY spectrum of **5** in DMSO-d_6/D_2O 10:90, there were two obvious symmetrical cross peaks between proton H_e of triazole group and protons H_b of TPE unit, demonstrating that triazole group and TPE unit were pulled to be close to each other (Fig. 4 and Fig. S16 in Supporting information). In addition,

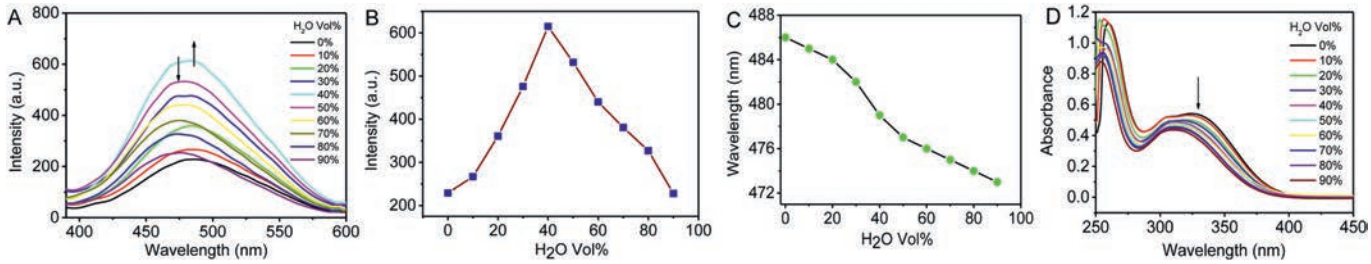

Fig. 2. Change in emission and absorption spectra with water fraction. (A) Change in emission spectra. (B) Change in emission intensity. (C) Change in emission maximum wavelength. (D) Change in absorption spectra. **[5]** = 1.0×10^{-4} mol/L, λ_{ex} = 342 nm, em/ex slits = 5/5.

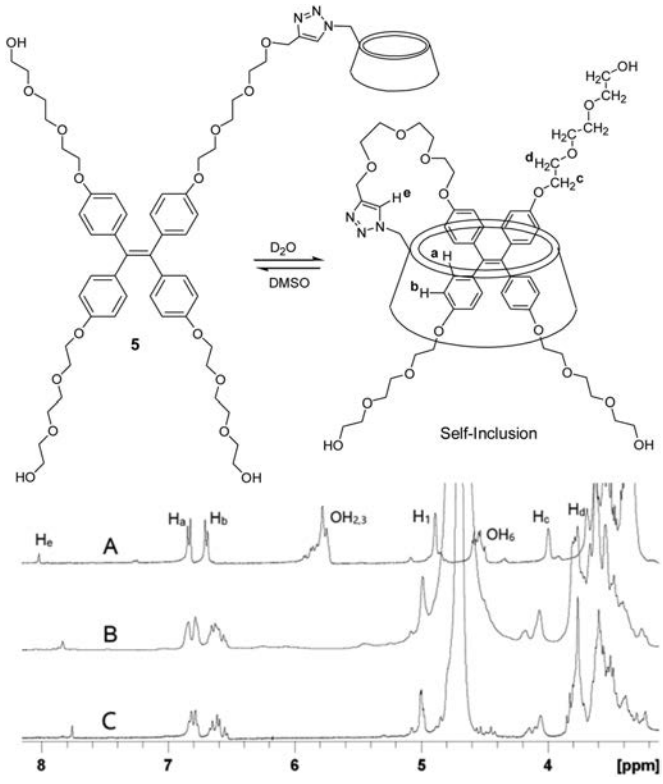

Fig. 3. The ^{1}H NMR spectra of conjugate **5** in a mixed solvent of DMSO-d_6/D_2O 10:90. **[5]** = 1.0 mmol/L; D_2O% in the mixed solvent = 0% (A), 60% (B), and 90% (C).

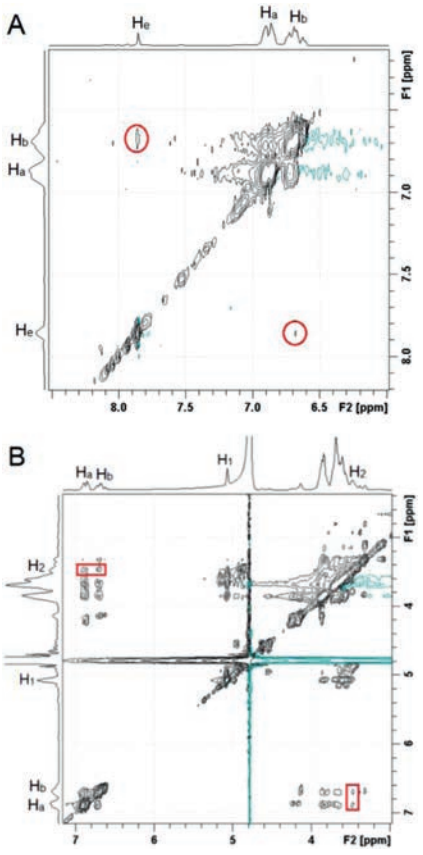

Fig. 4. Partial 2D NMR NOESY spectra of **5** in DMSO-d_6/D_2O 10:90. **[5]** = 2.0 mmol/L. The red cycles and boxes indicated the cross-peaks.

proton H_2 of γ-CD unit, which showed a strong cross-peak with H_1 of γ-CD unit because they were neighboring each other, displayed NOE signals with protons H_a and H_b of TPE unit, suggesting that the TPE unit was inserted into γ-CD cycle. Therefore, 2D NMR NOESY spectrum of **5** confirmed that its TPE unit was included into the cavity of the γ-CD unit.

To confirm that the TPE unit entered into the CD cavity of the same molecule or other conjugate molecule, the ^{1}H NMR spectra under gradual dilution condition were measured. It was observed that the chemical shift and the signal patterns of all protons of the conjugate **5** in DMSO-d_6/D_2O 10:90 had no any change with dilution (Fig. S17 in Supporting information). Therefore, the conjugate did not form dimer or multimers but produced self-inclusion compound through intermolecular host-guest interactions.

With the confirmation for the formation of self-inclusion compound, the unusual phenomenon of fluorescence change of conjugate **5** with water fraction could be explained. When the water was added by less than 40%, the aggregation was increased with water so that the fluorescence gradually increased. In the range of larger than 40% water fraction, the molecules of the conjugate was not only continued to aggregate but also start to form self-inclusion compound in the presence of a large amount of water. As a self-inclusion compound, the electron-rich TPE unit was not far away from, but was close to the triazole ring bearing nitrogen atoms that possessed lone par electrons, and a PET process [23,24] from nitrogen atoms of triaole ring to TPE unit at excited state could be efficiently realized (Fig. 5). After one of a pair of electrons in HOMO π-orbital was excited by UV light and transmitted to LUMO π-orbital of TPE unit, one of lone pair electrons in non-bonded orbital at the nitrogen atom of triazole ring transferred into the HOMO π-orbital of the TPE unit at excited state. As result, the excited electron at LUMO π-orbital was not able to transmit back to the HOMO π-orbital but instead back to non-bonded orbital at the nitrogen atom, which resulted in non-radiative releasing. Consequently, the fluorescence of the TPE unit was quenched. As more water was added, more self-inclusion compounds formed and resulted in more quenching, which even excessed AIE fluorescence enhancement. Therefore, the fluorescence was gradually

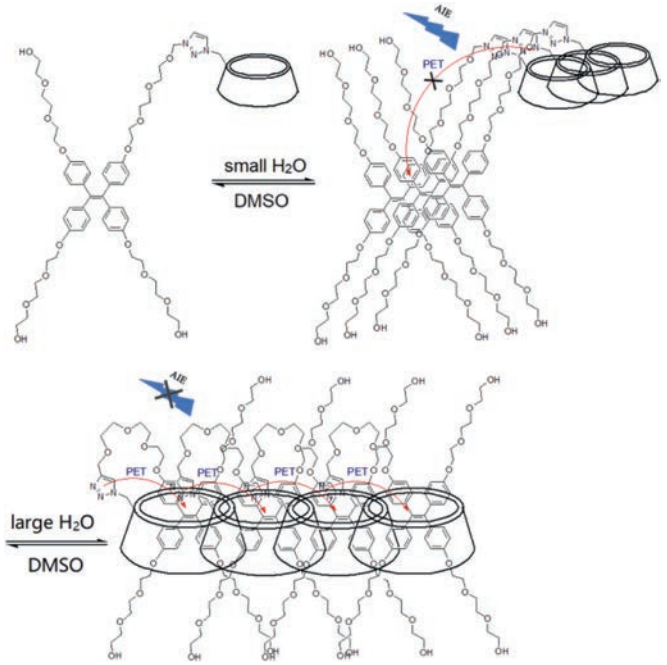

Fig. 5. The schematic diagram for kinetic equilibrium between AIE and PET process.

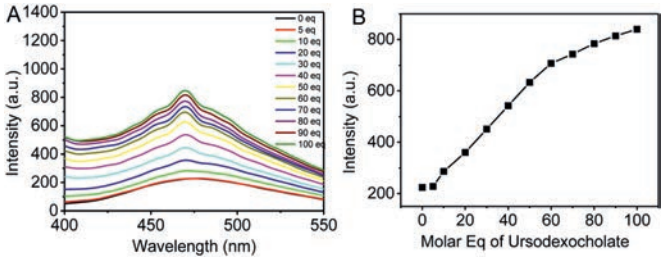

Fig. 6. Change in the fluorescence spectra (A) and fluorescence intensity (B) of compound **5** in DMSO-H_2O 10:90 with addition of potassium ursodeoxycholate. [**5**] = 1.0 × 10^{-4} mol/L, λ_{ex} = 342 nm, em/ex slits = 5/5.

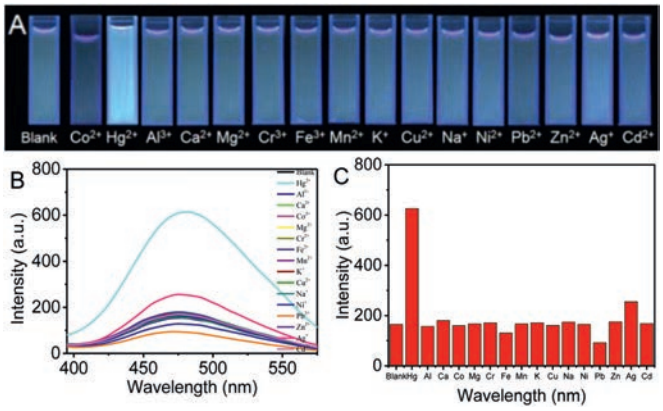

Fig. 7. (A) Photos under a portable 365 nm lamp and (B) fluorescence spectra of a mixture of **5** and metal ions in DMSO/H_2O 5:95. (C) Fluorescence intensity change with metal ions. **[5]** = 5.0 × 10^{-5} mol/L, [M^{n+}] = 1.0 × 10^{-4} mol/L, λ_{ex} = 342 nm, em/ex slits = 5/5.

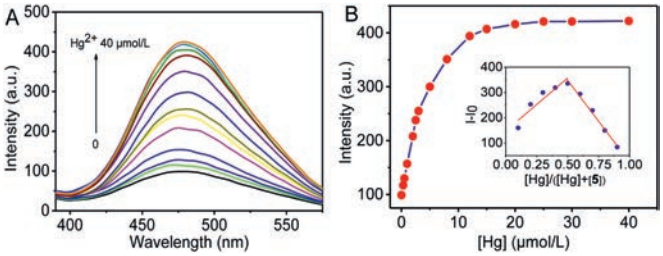

Fig. 8. Change in fluorescence spectra (A) and fluorescence intensity (B) of **5** in DMSO-H_2O 5:95 with concentration of Hg^{2+}. Inset, Job's plot for fluorescence titration of **5** with Hg^{2+}. **[5]** = 2.5 × 10^{-5} mol/L, [Hg^{2+}] = 0, 0.3, 0.5, 1, 2, 2.5, 3, 5, 8, 12, 15, 20, 25, 30, 40 μmol/L, λ_{ex} = 342 nm, em/ex slits = 5/5. I_0 and I denote the fluorescence intensity of **5** without and with addition of Hg^{2+} ions, respectively.

decreased with water in a range of more than 40% fraction. Meanwhile, upon aggregation and formation of more self-inclusion compounds, TPE unit became more twisted due to more intermolecular interactions and confining in CD cavity, the emission and absorption wavelength displayed obvious hypsochromic shift.

In order to further testify the PET mechanism of the self-inclusion compound, other guest potassium ursodeoxycholate that could be included by γ-CD was added into the solution of **5** in DMSO/H_2O 10:90. Interestingly, although the potassium ursodeoxycholate was non-emitting, the fluorescence intensity was gradually increased with continued addition of ursodeoxycholate. The increased intensity after addition of the potassium ursodeoxycholate was almost equal to the decreased magnitude that was aroused by PET quenching (Fig. 6). This test confirmed that PET process truly occurred.

Due to bearing multiple nitrogen and multiple oxygen atoms, the conjugate **5** should have interaction with some metal ions by coordination and would lead to the fluorescence change. Very unexpectedly, when metal ions including Fe^{2+}, Co^{2+}, Ni^{2+}, Zn^{2+}, Cu^{2+}, Cd^{2+}, Hg^{2+}, Mn^{2+}, Ag^+, Cr^{3+}, Pb^{2+}, Al^{3+}, Ca^{2+}, Mg^{2+}, K^+ and Na^+ as chloride except Ag^+ which was nitrate were added into the 5.0 × 10^{-5} mol/L solution of **5** in DMSO/H_2O 5:95, respectively, only Hg^{2+} could arouse fluorescence enhancement that could be observed by naked eyes and other metal ions almost caused no change (Fig. 7). In emission spectra of the mixtures, Hg^{2+} truly made the fluorescence significant increase by 3.8 folds while Ag^+ only aroused 1.5 folds increases. In contrast, Fe^{2+} and Pb^{2+} resulted in a little decrease of fluorescence intensity while Co^{2+}, Ni^{2+}, Zn^{2+}, Cu^{2+}, Cd^{2+}, Mn^{2+}, Cr^{3+}, Al^{3+}, Ca^{2+}, Mg^{2+}, K^+ and Na^+ almost had no effect on the fluorescence.

To know the effect of Hg^{2+} concentration on the fluorescence of **5**, fluorescence titration of **5** with Hg^{2+} was carried out. As shown in Fig. 8, the intensity was increased with Hg^{2+} concentration. In the range of less than 0.25 molar equivalents of mercury ion, the intensity was linearly increased with mercury concentration. After 1 equiv. of mercury ions were added, the intensity was not further increased and the change was beginning to level off (Fig. 8). The largest fluorescence enhancement was up to 4.26 times. By Job's plot of the fluorescence titration, the largest intensity difference appeared at [Hg]/([Hg]+[**5**]) = 0.5, so that the coordination ratio of **5** to mercury ion was 1:1. According to the Benesi–Hildebrand formula [25], $1/(I-I_0) = 1/((I_{max}-I_0)K[Hg^{2+}])+1/(I_{max}-I_0)$, in which I_{max} and I_0 denoted the maximum fluorescent intensity after addition of Hg^{2+} and without Hg^{2+}, respectively, and I_{max} denoted the maximum fluorescent intensity that did not further increased when more Hg^{2+} was added, the calculated coordination constant K was 1.86 × 10^5 L/mol (Fig. S18 in Supporting information). At the smallest Hg^{2+} concentration (3.0 × 10^{-6} mol/L) that aroused fluorescence increase, 11 samples were prepared and a standard deviation was obtained. According to detection limit = 3 × σ/k (σ, standard deviation; k, slope of the fitted straight line in the range of small concentration of Hg^{2+}), the calculated detection limit was 1.08 μmol/L.

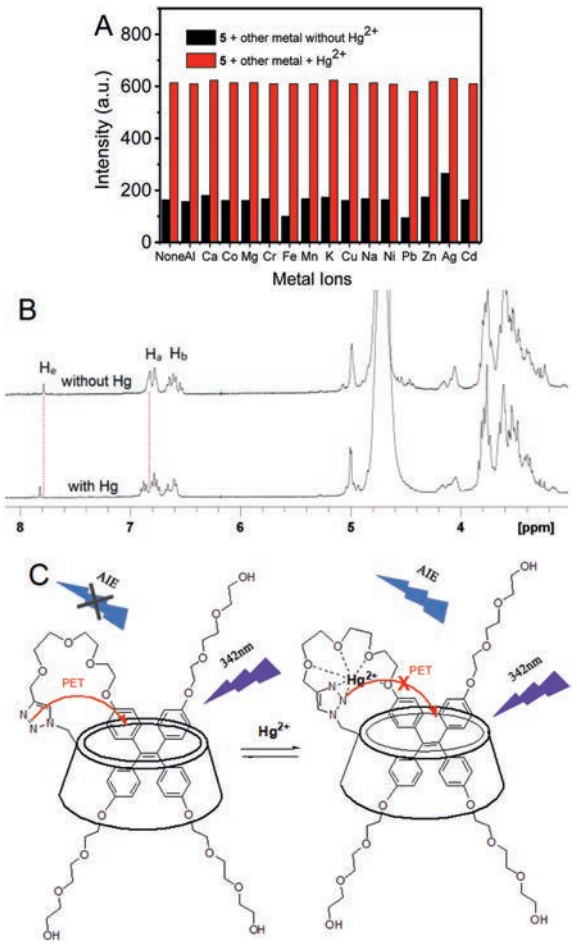

Fig. 9. (A) Change in the fluorescence intensity of a mixture of **5** and metal ions with and without Hg^{2+} in DMSO-H_2O 5:95. **[5]** = 5.0 × 10^{-5} mol/L, $[M^{n+}] = [Hg^{2+}] = 2.5 \times 10^{-4}$ mol/L, λ_{ex} = 342 nm, em/ex slits= 5/5. (B) The ^1H NMR spectra of **5** in DMSO-d_6/D_2O 10:90 with and without Hg^{2+}. **[5]** = 1.0 mmol/L, $[Hg^{2+}]$ 1.0 mmol/L. (C) Schematic diagram of blockage of PET process by Hg^{2+}.

In addition, the interference of other metal ions with the detection of Hg^{2+} was measured. As shown in Fig. 9A, in the presence of other metal ions, the increased fluorescence intensity by a mixture of Hg^{2+} and other metal ion was almost the same as the intensity aroused only by Hg^{2+}, demonstrating that other metal ions did not interfere with the detection of Hg^{2+}. Especially, although Ag^+ also gave rise to a little emission enhancement, the intensity of Ag^+ and Hg^{2+} mixture was almost equal to the intensity aroused by only Hg^{2+}, suggesting no effect of Ag^+ on Hg^{2+}. Strikingly, the most convenient and highly harmful metal ions, Cd^{2+}, Cr^{3+} and Pb^{2+}, also did not affect mercury detection. In addition, the effect of the counter ions on the detection of mercury ions was also tested and no effect was found (Fig. S19 in Supporting information).

To make insight into the binding mechanism of Hg^{2+} to conjugate, the comparison of ^1H NMR of **5** with and without addition of mercury ion was made. As shown in Fig. 9B, in the presence of Hg^{2+}, while the signal of triazole proton had a distinct lowfield shift of about 0.035 ppm, the TPE protons not only displayed lowfield shift of up to 0.076 ppm but also more doublet signals appeared. Therefore, the Hg^{2+} should be bound between triazole ring and phenoxy substitute of TPE unit. After coordination of Hg^{2+} to nitrogen atoms of triazole ring, the PET process from nitrogen atoms of triaozle to TPE unit was inactive and made the fluorescence recovery. Meanwhile, the *pseudo*-crown ether formed by the self-inclusion of the conjugate had a suitable size of cavity to accommodate mercury ion rather than other metal ions, so that the selectivity was very high (Fig. 9C). Other ions, especially the most convenient and highly toxic Pb^{2+}, Cd^{2+} and Cr^{3+} ions showed no response to this conjugate, displaying very exceptional result in selectivity. To the best of our knowledge, by forming *pseudo*-crown ether in self-inclusion compound to get selective sensors is not reported up to now, although the combination of AIE and PET effects have been exploited in chemo/biosensors [26–28].

In conclusion, a new TPE-CD conjugate with a spacer of long triethylene glycol and triazole was designed and synthesized. This conjugate could be transferred from stretched out structure to folded self-inclusion compound in the presence of large amount of water. Meanwhile, a supramolecular crown ether macrocycle was formed in the self-inclusion compound. Due to PET process from nitrogen atoms of triaozle to TPE unit, the AIE effect of the conjugate was attenuated and emitted weak fluorescence. After addition of metal ions, only the mercury ions could selectively coordinate to the cavity of supramolecular crown ether due to right size match of mercury ion with the cavity, and resulted in fluorescence enhancement. Therefore, this conjugate displayed a great potential for selective detection of mercury ions in water. This is the first time for disclosing the PET phenomenon in AIE host-guest chemistry. This result provided a new access to sensors with highly selectivity for analysis of metal ions by formation of supramolecular crown ether.

Declaration of competing interest

The authors declare that they have no known competing financial interests or personal relationships that could have appeared to influence the work reported in this paper.

Acknowledgments

The authors thank National Natural Science Foundation of China (Nos. 91856125 and 21673089) and HUST Graduate Innovation Fund for financial support, and thank the Analytical and Testing Centre at Huazhong University of Science and Technology for measurement.

Supplementary materials

Supplementary material associated with this article can be found, in the online version, at doi:10.1016/j.cclet.2021.08.072.

References

[1] J. Mei, N.L. Leung, R.T. Kwok, et al., Chem. Rev. 115 (2015) 11718–11940.
[2] H.T. Feng, Y.X. Yuan, J.B. Xiong, et al., Chem. Soc. Rev. 47 (2018) 7452–7476.
[3] M. Hu, H.T. Feng, Y.X. Yuan, et al., Coord. Chem. Rev. 416 (2020) 213329.
[4] H.T. Feng, J.B. Xiong, J. Luo, et al., Chem. Eur. J. 23 (2017) 644–651.
[5] M. Hu, Y.X. Yuan, W. Wang, et al., Nat. Commun. 11 (2020) 161.
[6] W.Z. Xie, H.C. Zhang, Y.S. Zheng, J. Mater. Chem. C 5 (2017) 10462–10468.
[7] Y.X. Yuan, M. Hu, K.R. Zhang, et al., Mater. Horiz. 7 (2020) 3209–3216.
[8] H.J. Kim, M.H. Lee, L. Mutihac, et al., Chem. Soc. Rev. 41 (2012) 1173–1190.
[9] X. Wang, J. Hu, T. Liu, et al., J. Mater. Chem. 22 (2012) 8622–8628.
[10] W. Bai, Z. Wang, J. Tong, et al., Chem. Commun. 51 (2015) 1089–1091.
[11] L. He, X. Liu, J. Liang, et al., Chem. Commun. 51 (2015) 7148–7151.
[12] S. Jiang, X. Hu, J. Qiu, et al., Analyst 144 (2019) 2662–2669.
[13] S. Song, Y.S. Zheng, Org. Lett. 15 (2013) 820–823.
[14] L. Zhang, W. Hu, L. Yu, Y. Wang, Chem. Commun. 51 (2015) 4298–4301.
[15] X. Huang, M. Lan, J. Wang, et al., Biosens. Bioelectron. 169 (2020) 112655.
[16] S. Fu, X. Su, M. Li, et al., Adv. Sci. 7 (2020) 2001909.
[17] P. Wei, Z. Li, J.X. Zhang, et al., Chem. Mater. 31 (2019) 1092–1100.
[18] H.T. Feng, Y. Li, X. Duan, et al., J. Am. Chem. Soc. 142 (2020) 15966–15974.
[19] C. Chen, X. Ni, H.W. Tian, et al., Angew. Chem. Int. Ed. 59 (2020) 10008–10012.
[20] V.G. Naik, V. Kumar, A.C. Bhasikuttan, et al., ACS Appl. Bio Mater. 4 (2021) 1813–1822.

[21] H. Liu, Z. Zhang, Y. Zhao, et al., J. Mater. Chem. B 7 (2019) 1435–1441.
[22] S. Song, H.F. Zheng, D.M. Li, et al., Org. Lett. 16 (2014) 2170–2173.
[23] J.S. Kim, D.T. Quang, Chem. Rev. 107 (2007) 3780–3799.
[24] X. Tian, L.C. Murfin, L. Wu, et al., Chem. Sci. 12 (2021) 3406–3426.
[25] J. Li, Y. Chen, T. Chen, et al., Sens. Actuat. B 268 (2018) 446–455.
[26] Q. Li, X. Wu, X. Huang, et al., ACS Appl. Mater. Interfaces 10 (2018) 3801–3809.
[27] S. Chen, S. Jiang, H. Guo, F. Yang, Spetrochim. Acta A 248 (2021) 119191.
[28] F. Zhang, C. Lu, M. Wang, et al., ACS Sens. 3 (2018) 304–312.